Journal of the Serbian Chemical Society
JSCS-info@shd.org.rs • www.shd.org.rs/JSCS

ACCEPTED MANUSCRIPT

Journal of the Serbian Chemical Society
JSCS-info@shd.org.rs • www.shd.org.rs/JSCS
J. Serb. Chem. Soc. **00(0)** 1-18 (2025)
JSCS–13409
Original scientific paper
Published DD MM, 2025

Sustainable synthesis of silver nanoparticles on cotton gauze for enhanced antibacterial properties

DARKA D. MARKOVIĆ[1]*, VANJA B. TADIĆ[2], ANA R. ŽUGIĆ[2] AND MAJA M. RADETIĆ[3]

[1]*University of Belgrade, Vinča Institute of Nuclear Sciences- National Institute of the Republic of Serbia, Mihajla Petrovića Alasa 12-14, Belgrade, 11351, Serbia,* [2]*University of Belgrade, Institute for Medical Plant Research "Dr Josif Pančić", Tadeuša Košćuška 1, 11000 Belgrade, Serbia, and* [3]*University of Belgrade, Faculty of Technology and Metallurgy, Karnegijeva 4, 11000 Belgrade, Serbia.*

(Received 3 June; revised 15 July; accepted 13 September 2025)

Abstract: Wound protection is a critical step in preventing or reducing infections, as well as in transmitting infections between patients. Wound dressings are essential medical products that cover wounds and facilitate healing. The present study examines the possibility of using Ag nanoparticles (NPs) to impart antibacterial activity to cotton gauze, a commonly used disposable wound dressing material. The *in situ* synthesis of Ag-based NPs on cotton gauze was achieved using extracts from *Populus x euramericana* (PE) and *Ailanthus altissima (Mill.) Swingle* (AA) leaves. Major phytochemical compounds in the extracts were quantified using HPLC. FESEM and EDS mapping analyses confirmed the presence of Ag-based NPs across the fibre surfaces on both samples. The average size of NPs synthesized in the presence of PE and AA extracts was 88±26 nm and 82±23 nm, respectively. A comparable amount of silver was found in the sample obtained with PE (14.22±0.23 μmol/g) and in the sample synthesized using AA extract (13.63±1.40 μmol/g). The synthesized samples achieved maximum bacterial reduction against Gram-negative bacteria *Escherichia coli* and Gram-positive *Staphylococcus aureus*.

Keywords: cotton gauze; Ag nanoparticles; plant extracts; green synthesis; antibacterial activity.

INTRODUCTION

Skin plays an important role in protecting the body from harmful external factors.[1-2] Diabetes, diseases, accidents, or burns can all damage the skin and cause wounds, as can minor cuts and surgical procedures.[3] Chronic wounds are usually caused by infection, while acute wounds are sometimes prone to infection. Surgical

* Corresponding author. E-mail: darka.markovic@vin.bg.ac.rs
https://doi.org/10.2298/JSC250603074M

wounds are especially vulnerable and can be colonised by a variety of bacteria, such as *Staphylococcus aureus, Pseudomonas aeruginosa, Escherichia coli, Klebsiella spp.,* and *Enterobacter spp*.[4-6] These microorganisms frequently cause wound infections that can progress to sepsis, pneumonia, or meningitis in patients.[7] Hence, wound management has been a big challenge in medicine worldwide. Wound protection is an important step in preventing or reducing infections, as well as in transmitting infections between patients.[8-9] Wound dressings are crucial medical products that cover wounds and support healing.[1] Cotton-based medical gauze is a type of sterile, disposable dressing that is commonly used to treat wounds due to its softness, breathability, affordability, and lack of skin irritation.[2,10] The primary issue with cotton gauze is that it cannot prevent or treat infections because bacteria in humid environments can readily stick to the surface of hydrophilic cotton fibers, enter the fibers and may create a biofilm, which acts as a reservoir for the growth of pathogens and poses a health risk to humans.[10] Consequently, antimicrobial treatments are crucial for mitigating and preventing microbial proliferation. Antimicrobial agents for antimicrobial finishing of textile materials can be classified as organic, inorganic, or natural.[11] The more studied types of antimicrobial agents include biguanides, triclosan, quaternary ammonium salts, metallic silver, zinc oxide, triclosan, herbal extracts and certain natural and metal complex colors.[12-16] Owing to their excellent antimicrobial activity against a wide range of microorganisms and low cytotoxicity, silver nanoparticles (Ag NPs) have received much interest. Among various methods that have been used for the synthesis of Ag NPs, such as microwave-assisted reduction, salt reduction, reverse micelles, and ultrasonic irradiation, the widely used and investigated method is the reduction of silver nitrate in aqueous solution, using a reducing agent such as sodium borohydride ($NaBH_4$) or hydrazine.[17-18] Exploitation of conventional strong reducing agents enables the synthesis of smaller NPs, but the toxicity of such reducing agents has prompted research into more environmentally friendly routes.

Green synthesis of Ag NPs includes utilising bacteria, fungi, enzymes, polysaccharides, and plant extracts as reducing agents for metal ions.[17-18] Owing to its natural abundance and low cost, various plants and their parts (roots, leaves, seeds, fruits) have been extensively investigated in the synthesis of colloidal Ag NPs.[19] Despite the substantial studies on the green synthesis of Ag NPs, research on the green synthesis of these NPs on textile fibers remains limited. One possible explanation might be the lack of adequate reproducibility in terms of NPs shape, size and stability due to the variability in chemical composition (e.g. phenolic compounds and flavonoids), which is closely tied to geographical location, weather and environmental conditions. Moreover, the use of plants can be complicated because they are seasonal. In terms of ex situ strategies for

synthesizing Ag NPs, it is commonly difficult to achieve monodisperse NPs, which are beneficial for multiple applications, including textiles.[20]

Sodium alginate and aloe vera inkjet print onto cotton fabric were used as a sustainable reducing agent for *in situ* synthesis of Ag NPs.[21] Antimicrobial cotton fabric was fabricated using whey protein isolate as both a reducing agent and stabilizer for Ag NPs.[17] *Spirulina*, a microalga rich in proteins, polysaccharides, vitamins, and phenolic could be successfully employed for antimicrobial finishing of cotton with Ag NPs.[18] Maghimaa *et al*. synthesized the metallic Ag NPs from the aqueous extract of *Curcuma longa* L. leaf and evaluated their antimicrobial and wound healing potential of Ag NPs-coated cotton fabric.[22] It is shown that Black rice (*Oryza sativa* L.) could be used for *in situ* green synthesis of Ag NPs on carboxymethyl chitosan modified cotton substrate.[23] *In situ* phytosynthesis of Ag NPs on cotton fabric was also performed using extracts of plant materials from food waste (green tea leaves (*Camellia sinensis* (L.) Kuntze), avocado seed (*Persea americana* Mill.) and pomegranate peel (*Punica granatum* L.) and invasive alien species (the Japanese knotweed rhizome (*Fallopia japonica* Houtt.), the staghorn sumac fruit (*Rhus typhina* L.), and goldenrod flowers (*Solidago canadensis* L.)).[24] Štular *et al*. synthesized Ag NPs in the presence of sumac leaf extract onto polysiloxane modified cellulose fibres.[25]

Our previous studies have revealed that extracts of *Paliurus spina-christi* Mill., *Juglans regia* L., *Humulus lupulus* L., and *Sambucus nigra* L. could be successfully used for *in situ* synthesis of Ag-based NPs on cotton fabric modified with citric acid.[26] Pomegranate peel extract (*P. granatum*) was also utilised for the simple *in situ* synthesis of Ag-based NPs on chitosan-modified viscose fibers.[27] Considering that a variety of phytochemicals found in different plant extracts may serve as reducing, stabilizing and capping agents, our intention was to extend previous research by utilizing the extract of cultivated hybrid *Populus x euramericana* (Dode) Guinier I-214, Salicaceae (buds) and weed species *Ailanthus altissima* (Mill.) Swingle, Simaroubaceae (leaves) for *in situ* synthesis of Ag-based NPs on cotton gauze to impart antibacterial activity. *P. euramericana* is a fast-growing plantation tree that is extensively exploited in the wood industry, but thin branches with buds are regarded as waste. On the other hand, *A. altissima* (Tree-of-heaven) is an invasive species that causes serious damage to the ecosystem, economy, and public health in the United States and Europe.[28] To the best of our knowledge, there is only one paper that has addressed the exploitation of bark extract *A. altissima* for the synthesis of Ag NPs.[29] Furthermore, to our knowledge, no research has been conducted on the *in situ* synthesis of Ag-based nanoparticles on textile substrates using extracts derived from *P. euramericana* and *A. altissima*. Major phytochemical compounds in the extract were quantified by HPLC. Morphological and chemical changes on the fiber surface were assessed by FESEM and FTIR, respectively. The total content of silver and the released

amounts of Ag^+ ions were quantified by AAS. Antibacterial activity of cotton gauze with Ag-based NPs was tested against Gram-negative bacteria *E. coli* and Gram-positive bacteria *S. aureus*.

EXPERIMENTAL

Materials

Populus x euramericana (Dode) Guinier I-214, Salicaceae was provided by "Srbija sume", Belgrade in March 2024, while *Ailanthus altissima* (Mill.) Swingle, Simaroubaceae was collected in the forest of Košutnjak (N: 44°46′34″, E: 20°25′56″) in Belgrade at the beginning of June 2024. The voucher specimens were deposited and identification was performed at the Faculty of Forestry, University of Belgrade.

Nitric acid and sodium chloride were purchased from Zorka Pharma, Serbia. Centrohem, Serbia, provided silver nitrate. The microbial inoculum was prepared in tryptone soya broth, agar, and yeast extract provided by Torlak, Serbia. Cotton gauze was supplied by Diva (Serbia) and used without further purification.

Preparation of plant extracts

The plants *P. euramericana* (PE) and *A. altissima* (AA) were selected for the synthesis of Ag-based NPs. The plant extracts were prepared in the form of decocts by adding 6.00 g of buds or leaves (previously milled) to 100 mL of distilled water. The vessel containing the extract was sealed and heated to 80ºC for 1 h. Prepared extracts/decocts were filtered and immediately used for the synthesis of Ag-based NPs.

HPLC analysis of PE and AA leaves decoction

Comprehensive analyses of the tested decoctions, from the aspect of their chemical profile, were achieved using HPLC analysis. "Fingerprinting" of the investigated samples was carried out using a 1200 HPLC system (Agilent Technologies) equipped with a Phenomenex, HydroRP 80, 150x4.6 column using two mobile phases (phase A being 0.1 M solution of phosphoric acid, and phase B pure acetonitrile). Flow rate was 0.800 mL/min, with photodiode-array (PDA) detection (UV at 260). Best peak separation was achieved using the following combination: 2% B (0 min); 2-10% B (0-5 min); 10% B (5-15 min), 10-15% B (15-20 min) and 15-60% (20-45 min). For poplar buds, the slightly modified method was used, namely the flow rate was 1.00 mL/min, with photodiode-array (PDA) detection (UV at 360 nm, for catechin at 260 nm). The elution was performed 11% B (0 min);11-25% B (0-5 min); 25% B (5-10 min), 25-40% B (10-20 min), 40% B (20-35 min), 45-55% B (35-50 min) and 50-60% B (50-60 min). Before injection, the samples of PE and AA (c=24.6 and 8.6 mg/mL, respectively) were filtered through a PTFE membrane filter. For standards gallic acid, neochlorogenic acid, chlorogenic acid, procyanidin B1, catechin, caffeic acid, epigallocatechin gallate, p-coumaric acid, ferulic acid, taxifolin, rutin, 3,5-di-O-caffeoylquinic acid, naringin, rosmarinic acid, t-cinnamic acid, quercetin, pinobanksin, naringenin, pinocembrin, chrysin, syringic acid, myricitrin, ellagic acid, isoquercetin, quercitrin, kaempferol-3-O-glucoside, apigenin-7-O-glucoside, and diosmin (Chem Faces, China) used in the investigation, the concentrations were 0.07, 0.3, 0.42, 0.14, 0.40, 0.52, 0.32, 0.50, 0.43, 0.30, 0.44, 0.39, 0.28, 0.43, 0.58, 0.21, 0.20, 0.38, 0.46, 0.47, 0.19, 0.50, 0.34, 0.52, 0.28, 0.49, and 0.38 mg/mL, respectively. The injection volume of the standard solutions and the tested extract was 4 µL. Identification was based on overlay curves and the retention times. After spectra matching succeeded, results were confirmed by spiking with the respective standard to achieve a complete identification using the peak purity test. The peaks

that did not fulfil these requirements were not quantified. Quantification was performed through external calibration with the standard.

The total phenolic content was determined by the Folin–Ciocalteu method.[30] 100 µL of methanol solution of the investigated sample (starting concentration being 5.66 and 6.97 mg/mL, for heaven of tree and poplar, respectively) was mixed with 0.75 mL of 10-fold diluted Folin–Ciocalteu reagent and allowed to stand at 22 °C for 5 min; 0.75 mL of sodium bicarbonate (60 g/L) solution was added to mixture. After 90 min at 22 °C, absorbance was measured at 725 nm. Gallic acid (0–100 mg/L) was used for calibration of a standard curve. The calibration curve showed the linear regression at $R^2 > 0.99$, and the results are expressed as milligrams of gallic acid equivalents per g dry weight (DW). Triplicate measurements were taken and data were presented as mean ± standard deviation (SD).

The percentage content of tannins was calculated using the method described in the European Pharmacopoeia 11.0.[31] Briefly, the investigated extracts were treated with phosphomolybdotungstic reagent in an alkaline medium after and without treatment with hide powder reagent. The absorbance was measured by UV-VIS Spectrophotometer HP 8453 (Agilent Technologies, USA), at a max of 760 nm. The percentage content of tannins expressed as pyrogallol (%, w/w), was calculated from the difference in absorbance of total polyphenols (*A1*) and polyphenols not adsorbed by hide reagent (*A2*), using the following expression:

$$(62.5 \times (A1 - A2) \times m2) / (A3 \times m1) \quad (1)$$

where *m1* represents the mass of the sample to be examined, in grams; and *m2* and *A2* mass, in grams and the absorbance of pyrogallol, respectively. The results represent the mean of three determinations.

In situ synthesis of Ag-based NPs on the modified samples

One gram of cotton gauze (COG) was soaked in 30 mL of a 20 mM solution of $AgNO_3$ for one hour. Afterwards, the sample was rinsed two times with deionised water and put in the freshly prepared solution of plant extract. The synthesis step was conducted at 60 ºC for one hour. Subsequently, the samples were thoroughly rinsed with distilled water and left to dry at room temperature. Cotton gauze containing Ag-based NPs synthesized in the presence of PE and AA were marked as COG-Ag-PE and COG-Ag-AA, respectively. Simultaneously, COG samples were put in PE and CC extracts at 60 °C for one hour. After rinsing, samples were marked as COG-PE and COG-AA, respectively. The synthesis route is schematically presented in Fig. 1.

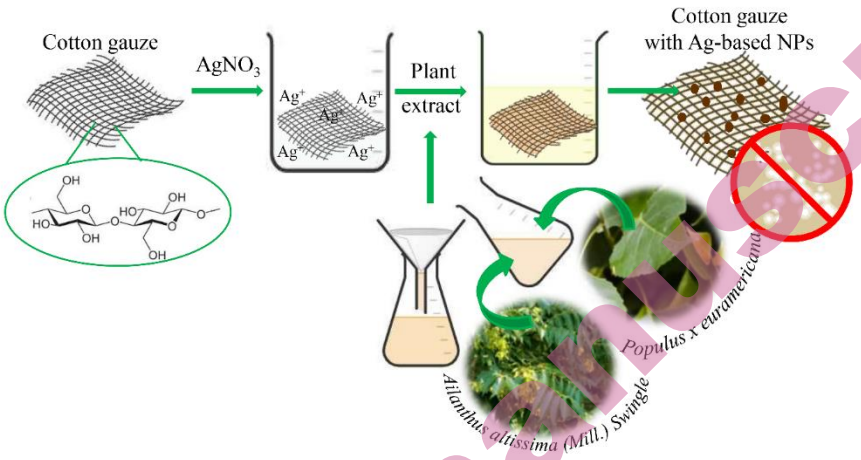

Fig. 1 Schematic presentation of green *in situ* synthesis of Ag-based NPs onto cotton gauze

FE-SEM analysis

The morphology of fibers with embedded Ag-based NPs, and the qualitative analysis of chemical composition and distribution of silver over the surface were investigated by field emission scanning electron microscopy equipped with an energy dispersive X–ray spectrometer (FESEM-EDS, FEI SCIOS 2 Dual Beam). The samples were recorded under high vacuum with an acceleration voltage of 7 kV. The EDS mapping acquisition time was 30 min. To define the size and size distribution of NPs, the obtained FESEM images were analysed using the open-access imaging software tool ImageJ.

FTIR analysis

Fourier transform infrared (FTIR) spectra of the COG, COG-PE, COG-AA, COG-Ag-PE, and COG-Ag-AA samples were recorded in the ATR mode using a Nicolet iS5 FTIR Spectrometer (Thermo Scientific) at 4 cm^{-1} resolution, in the wavenumber range 500 – 4000 cm^{-1}.

The total amount of Ag

The total amount of Ag in the samples was measured using atomic absorption spectroscopy (AAS). The measurements were conducted in absorption mode at a wavelength 328.1 nm. The COG-Ag-PE and COG-Ag-AA samples were immersed in a nitric acid solution (H_2O:HNO_3 1:2) and subsequently analysed using AAS after 24 hours.

Color measurements

The color coordinates of the samples, represented as CIE L*, a*, and b*, were measured utilising a Datacolor SF300 spectrophotometer under the D65 illuminant, employing the 10° standard observer.

Antibacterial test

Antibacterial activity of the samples with Ag-based NPs was tested against Gram-negative bacteria *E. coli* ATCC 25922 and Gram-positive bacteria *S. aureus* ATCC 25923 using a standard test method for determination of the antimicrobial activity of immobilised antimicrobial agents under dynamic contact conditions ASTM E 2149-01 (2001). Bacterial inoculums were cultivated in the tryptone soya broth (3 mL) supplemented with 0.6% w/v yeast

extracts at 37 °C and left for 18 h (late exponential stage of growth). Freshly grown bacterial cultures were diluted in sterile physiological saline solution to obtain the inoculum with an initial number of cells of *ca*. 10^7 CFU/mL. 50 mL of sterile physiological saline solution (pH 7.2) was inoculated with 0.5 mL of a bacterial inoculum. One gram of the control COG, COG-Ag-PE, and COG-Ag-AA samples (previously sterilised in an autoclave for 15 min) were placed in the flask with physiological saline solution and microorganisms at 37 °C and shaken for 2 and 24 hours. After these time intervals, 1 mL aliquots from the flask were taken and diluted with physiological saline solution, and 1 mL of the solution was placed onto a tryptone soya agar supplemented with 0.6 w/v% yeast extracts. After 24 hours of incubation at 37 °C, the zero time (initial number of bacteria colonies), 2 and 24 hours counts of viable bacteria were made.

The percentage of bacteria reduction (R, %) was calculated using the following equation:

$$R = \frac{C_0 - C}{C_0} \cdot 100 \quad (2)$$

where C_0 (CFU/mL – colony forming units) is the number of bacteria colonies on the control sample (COG) and C (CFU/mL) is the number of bacteria colonies on the fabric with Ag-based NPs.

Release study

To access the release capability of Ag^+ ions from the samples, 0.25 g of COG-Ag-PE and COG-Ag-AA were immersed in 25 mL of physiological saline solution (9 g/L NaCl) and maintained at a temperature of 37 ºC. The concentration of Ag^+ ions released was measured at intervals of 1, 3, 6 and 24 hours using AAS at a wavelength of 328.1 nm.

AAS analysis was also conducted to assess the concentration of Ag^+- ions that were released from COG-Ag-PE and COG-Ag-AA samples after 2 and 24 hours in a physiologically saline solution, under the conditions utilized in the antimicrobial test.

RESULTS AND DISCUSSION

Plants (leaves, flowers, seeds, stems, and roots) possess a high bioreduction potential owing to their varied reactive constituents, including polyphenols, terpenoids, proteins, reducing sugars, polysaccharides, and amino acids. Among these, phenols, proteins, saponins, and alkaloids are recognised as the most effective reducing, capping, and stabilising agents,[32] as they inhibit the growth and aggregation of Ag NPs in the solution. Fig. 2 presents the HPLC spectra of PE and AA water extracts decoction. Chemical composition of PE and AA decoction is revealed in Tables 1 and 2, respectively.

The aqueous leaf extracts of PE and AA are rich in various biomolecules/phytochemicals (Fig. 2). Tables 1 and 2 imply that the total phenolic content found in PE and AA extracts was 278.1 ± 2.15 and 247.15 ± 1.05 mg GAE/g, respectively. The total tannin content was 0.05 and 0.17% in PE and AA extracts, respectively. The HPLC analysis revealed the predominant presence of simple phenolic compounds, flavan-3-ols, flavanonols and polyphenolic acids (gallic acid, procyanidin B1, caffeic and rosmarinic acids, Figure 2a, Table I) in PE, while AA was rich in chlorogenic, syringic and ellagic acids (Figure 2b, Table II). Namely, comparing PE and AA, PE extract had higher content of total phenolic

compounds, represented by phenolic acids (rosmarinic, caffeic, and t-cinnamic acids) and gallic acid and flavan-3-ols derivatives (catechin, procyanidins), while AA extract, although rich in phenolic constituents, was less abundant in gallic and phenolic acids (the highest content was detected for chlorogenic and syringic acids). The flavonoids were detected in both investigated samples. These compounds can interact with the metal ion via the hydroxyl group (OH) and form metal NPs through the bioreduction process.[32] The presence of flavonoids and phenolic acids with hydroxyl and ketonic groups in the extract could be responsible for the formation of the metal nanoparticles. These compounds could be adsorbed on the surface of metal nanoparticles, possibly through π-electron interaction in the absence of other strong ligating agents.[33] Namely, tautomeric transformation of flavonoids and phenolic acids from enol to keto form is followed by release of reactive hydrogen atoms that can reduce Ag^{+} ions to Ag^{0}.[32]

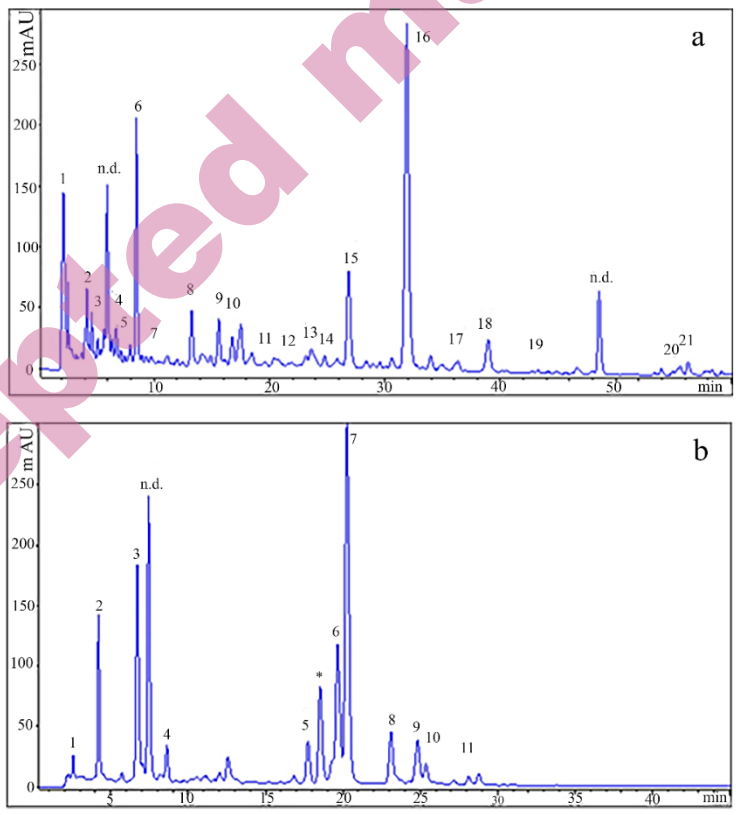

Fig. 2. HPLC chromatogram of (a) PE decoction recorded at 260 nm and (b) AA decoction recorded at 360 nm (the presented peak numbers correspond to compounds in Tables 1 and 2) (n.d.- not detected, * - ellagic acid derivative)

Table I. Chemical composition of PE decoct*

	Compound, mg g^{-1} DW extr**	*Populus x euramericana* (Dode) Guinier I-214, Salicaceae, bud *decoction*
1	*Gallic acid*	55.30±1.05
2	*Neochlorogenic acid*	7.46±0.38
3	*Procyanidin B1*	22.55±1.26
4	*Catechin*	6.42±0.22
5	*Chlorogenic acid*	4.83±0.12
6	*Caffeic acid*	20.15±1.01
7	*Epigallocatechin gallate*	1.15±0.05
8	*p-Coumaric acid*	6.04±0.19
9	*Ferulic acid*	5.39±0.15
10	*Taxifolin*	9.18±0.33
11	*Rutin*	0.75±0.02
12	*Quercitrin*	0.64±0.03
13	*3,5-di-O-caffeoylquinic acid*	1.98±0.09
14	*Naringin*	11.91±0.35
15	*Rosmarinic acid*	27.17±0.71
16	*t-Cinnamic acid*	15.48±0.44
17	*Quercetin*	0.80±0.02
18	*Pinobanksin*	17.32±0.63
19	*Naringenin*	0.76±0.02
20	*Pinocembrin*	5.06±0.09
21	*Chrysin*	0.11±0.01
	Total phenolic compounds mg GAE/g	278.1±2.15
	Tannin content (%)	0.05±0.01

*the type of the extract preparation, whose preparation was explained in the Methodology
**DW extr – dry weight of the analzyed extract

Table II. Chemical composition of AA decoct

	Compound, mg g^{-1} DW extr	*Ailanthus altissima* (Mill.) Swingle, Simaroubaceae leaf decoction
1	*Gallic acid*	6.07±0.02
2	*Neochlorogenic acid*	6.07±0.02
3	*Chlorogenic acid*	14.58±0.11
4	*Syringic acid*	21.17±0.21
5	*Myricitrin*	1.33±0.01
6	*Ellagic acid*	5.84±0.03
7	*Isoquercetin*	6.89±0.10
8	*Quercitrin*	1.71±0.03
9	*Kaempferol-3-O-glucoside*	0.96±0.02
10	*Apigenin-7-O-glucoside*	0.55±0.01
11	*Diosmin*	0.22±0.01
	Total phenolic compounds mg GAE/g	247.15±1.05
	Tannin content (%)	0.17±0.01

The initial analysis of the synthesis process for Ag-based nanoparticles was validated through visual confirmation of the COG sample's color shift from white to dark brown (Fig. 3a). It is well documented that biosynthesis of Ag-based NPs produces brown-colored solutions or solid samples.[25-26,32,34] Our recent study revealed that the *in situ* synthesis of Ag-based NPs using extracts from *P. spina-christi, J. regia, H. lupulus*, and *S. nigra* resulted in the coloration of cotton samples in various shades of brown.[26] Stular *et al*. reported that cotton samples coated with various concentrations of Ag NPs synthesized in the presence of sumac leaf extracts were colored in shades ranging from yellow to brown.[25] The color change was quantified by determining the CIE L*a*b* coordinates (Fig. 3b). Apparently, the color of the samples changed considerably after the synthesis of Ag-based NPs, resulting in darker reddish and more yellowish shades of the samples (Fig. 3a and 3b).

Fig. 3c illustrates the change in the shape of the reflectance curves after coating with plant extracts, and the biosynthesis of Ag-based NPs. The reflectance intensity and shape of the reflectance curve of COG altered after being treated with plant extracts, especially in the wavelength range of 400-500 nm. An additional decrease in reflectance intensity was observed after the *in situ* synthesis of Ag-based NPs. The shape of the reflectance curves for COG-Ag-PE and COG-Ag-AA is significantly different across the entire measuring range, particularly in the high-energy region, where a slight drop of reflectance intensity appeared. This suggests the emergence of the plasmon resonance band of Ag NPs at approximately 475 nm. Similar results were reported for the cotton fabric loaded with colloidal Ag NPs.[35]

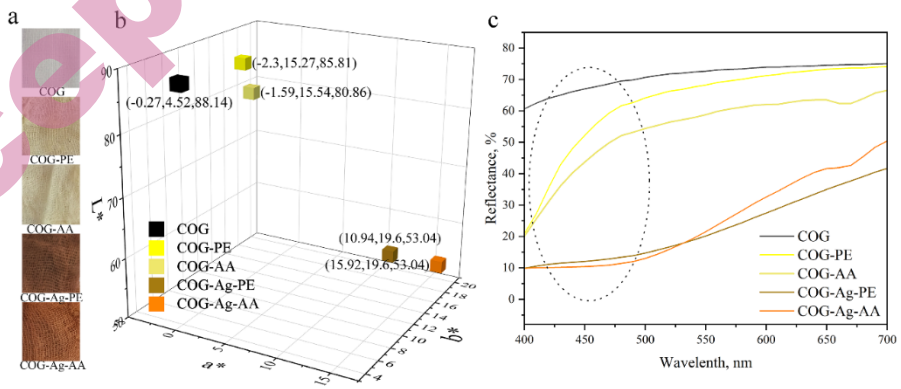

Fig. 3. The photographs, L*a*b* coordinates and reflectance spectra of the samples

ESEM was employed to verify the existence of Ag-based NPs on COG fibers. The FESEM micrographs and EDX element distribution mapping for the COG-Ag-PE and COG-Ag-AA samples are shown in Fig. 4 and Fig. 5, respectively.

Different colors were used to visually distinguish the presence of carbon (red), oxygen (green) and silver (cyan). FESEM micrographs indicate that spherical Ag-based NPs uniformly covered the surface of the COG-Ag-PE fibers (Fig. 4). The acquired silver maps further highlight the extent of silver coverage of the fiber surface. Fig. 4 also presents the size distribution of NPs across COG-Ag-PE fibers. Evidently, the size of the synthesized NPs was observed to vary between 20 and 177 nm, with an average size of 88 ± 26 nm. AAS analysis revealed that 14.22 ± 0.23 µmol of silver was found in one gram of the COG-Ag-PE sample (1.53±0.02 mg/g).

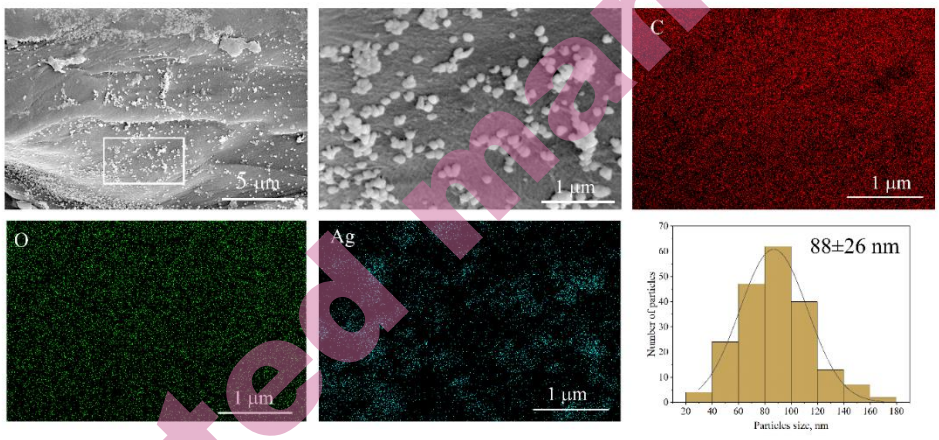

Fig. 4. FESEM micrographs, mapping and particle size distribution of COG-Ag-PE sample

In comparison to the COG-Ag-PE surface (Fig. 4), a smaller number of spherical NPs was visible on the COG-Ag-AA surface (Fig. 5). Additionally, the size distribution demonstrated the presence of smaller NPs ranging from 29 to 140 nm, with a mean size of 82 ± 23 nm. AAS analysis showed that the total content of silver in the COG-Ag-AA sample was 13.63 ± 1.40 µmol/g (1.47 ± 0.15 mg/g). Given that the total silver content in COG-Ag-PE and COG-Ag-AA is comparable, the reduced quantity of synthesized NPs in the COG-Ag-AA sample (Fig. 5) may indicate that a portion of Ag^+ ions was merely adsorbed onto the cotton fibers. This may be attributed to the concentration of gallic acid, recognized as an effective reducing and stabilizing agent,[36] which was found to be nearly nine times lower in the AA extract compared to that in the PE extract (Table I and II). Nevertheless, an in-depth investigation into the effect of gallic acid on the formation of Cu-based NPs demonstrated that a single component in the extract cannot solely account for the overall results; rather, it is the synergistic interaction of the various phytochemicals present that plays a crucial role.[36] In general, the variation in the overall quantity of Ag NPs is the consequence of the differing total phenolic

content observed in the samples (Tables 1 and 2). Larger amounts of silver (17 - 27 µmol/g) on the cotton samples were accomplished in our previous study, where *P. spina-christi, J. regia, H. lupulus* and *S. nigra* leaves extracts were employed for *in situ* synthesis of Ag-based NPs.[26] The observed outcomes may be attributed to prior modifications of cotton using citric acid, which introduces carboxyl groups that improve the material's capacity to adsorb Ag^+ ions. The size distribution and the overall quantity of silver obtained in this research fell within the findings reported by Štular *et al*.[25]

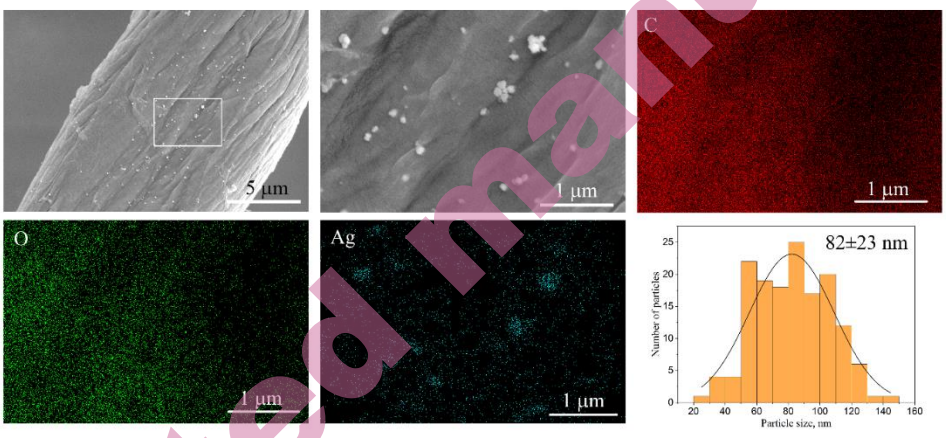

Fig. 5. FESEM micrographs, mapping and particle size distribution of COG-Ag-Aof the COG, COG-PE, COG-AA, COG-AG-PE, and COG-Ag-AA are shown in Fig. 6. The bands characteristic of cellulose are visible in all spectra. The band located between 3500-3200 cm^{-1} is ascribed to the hydrogen-bonded O–H stretching in cellulose. The bands centred at 2898 cm^{-1} and 1427, 1364, 1315 and 1280 cm^{-1} are related to C–H asymmetric stretching, C–H in-plane bending vibrations, C–H bending vibrations, C–H wagging vibrations and C–H deformation stretch vibrations, respectively. The OH in-plane bending vibration is located at 1203 cm^{-1}. The band centred at 1640 cm^{-1} could be related to adsorbed water molecules. The bands at 1156,1105, 1050, 1031 correspond to asymmetric bridge C–O–C, asymmetric in-plane ring stretching and C–O stretching, respectively. The band at 900 cm^{-1} originates from asymmetric out-of-phase ring stretching at the C1–O–C4 glucosidic bond.[37] FTIR spectra of gauze loaded with herbal extracts are similar to those of the control gauze. Keeping in mind that herbal extracts are cellulose in origin, the overlapping of bands has occurred.

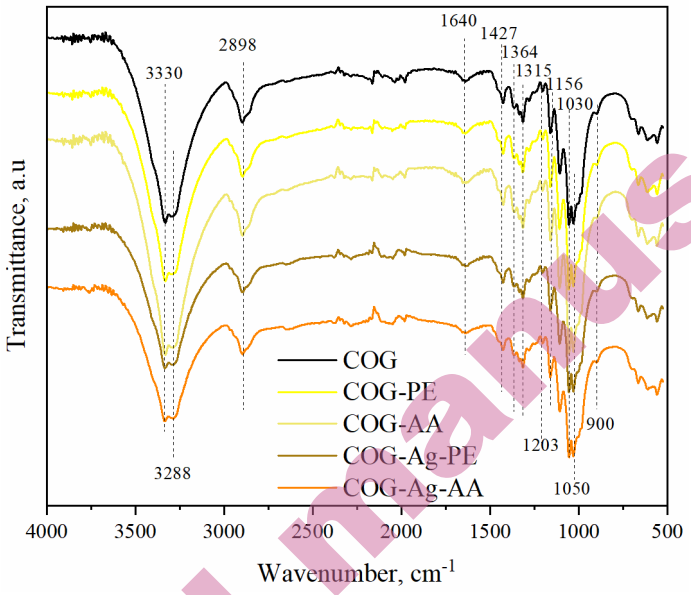

Fig. 6 FTIR spectra of COG, COG-PE, COG-AA, COG-Ag-PE and COG-Ag-AA samples

Table III summarises the results of antibacterial reduction of bacteria *E. coli* and *S. aureus* after 2 hours and 24 hours of contact with synthesized samples. The results indicated that COG and COG samples loaded only with plant extracts did not exhibit any antibacterial activity towards the investigated pathogens. The *in situ* synthesis of Ag-based NPs ensured a 99.9% reduction of bacteria *S. aureus* just after 2 hours of contact with the COG-Ag-PE sample. This sample did not provide sufficient reduction of bacteria *E. coli* after 2 hours of contact. However, a significant reduction of 99.9 % was achieved after 24 hours of contact. The COG-Ag-AA sample ensured a 98.9 % reduction of bacteria *S. aureus* after 2 hours of contact, and maximum bacteria reduction after 24 hours. The COG-Ag-AA sample provided a 99.9 % reduction of bacteria *E. coli* after 24 hours of contact. Both samples exhibited greater antibacterial activity against Gram-positive bacteria during shorter contact times than against Gram-negative bacteria, where bacteriostatic activity was attained. Despite differences in cell wall structure, it has been well known that Ag NPs have similar antibacterial activity against Gram-positive and Gram-negative bacteria.[38] Apparently, a higher silver content or a longer contact time is necessary for the complete inhibition of Gram-negative strains.

Several mechanisms for silver antibacterial activity have been postulated so far: i) absorption of free silver ions, which disrupts DNA replication and ATP synthesis; ii) production of reactive oxygen species (ROS) by Ag NPs and silver ions; and ii) Ag NPs may also cause direct damage of the cell membrane, which

could result in the leakage of cell contents.[38] In order to provide a more comprehensive understanding of the antibacterial effects of Ag-based NPs synthesized on cotton gauze, the quantity of silver leached from the sample during the antibacterial evaluation was measured. AAS analysis revealed that 2.33±0.05 µg/ml and 2.55±0.04 µg/ml of Ag^+-ions were released from the COG-Ag-AA sample after 2 and 24 hours, respectively. The COG-Ag-PE samples showed a similar trend of Ag^+ ions release, with 2.51±0.28 µg/ml and 2.54±0.01 µg/ml of Ag^+ ions released after 2 and 24 hours, respectively. The synthesis method, colloidal concentration, NPs size, and various other factors significantly affect the minimal inhibitory concentration (MIC) of Ag NPs. The estimated MIC values for Ag NPs against *E. coli* and *S. aureus* were observed to be in the range of 6.75-320 µg/ml and 13.5-80 µg/ml, respectively, varying according to the size of the NPs.[39] Moreover, the MIC for both microorganisms spans from 0.25 µg/ml to 400 µg/ml, depending on the synthesis method utilized.[39] Some studies indicated that the MIC of Ag NPs against *E. coli* varied from 5.087-8.8 µg/ml.[40] Another research revealed that the MIC of Ag NPs against *E. coli* was 3.38 mg/l and for *S. aureus* 13.5 mg/L.[41] Given that the reported MIC values are significantly higher than the concentration of Ag^+ ions released from the tested samples, it can be concluded that in our study direct contact with NPs plays a significant role in antibacterial action. Furthermore, the negligible difference observed in the concentrations of Ag^+ ions released after 2 and 24 hours supports this conclusion, demonstrating that the length of contact time plays a crucial role in the antibacterial effect.

TABLE III. Antibacterial activity of samples with Ag NPs

Sample	Bacteria							
	E. coli				*S. aureus*			
	2 h contact CFU/mL	R, %	24 h contact CFU/mL	R, %	2 h contact CFU/mL	R, %	24 h contact CFU/mL	R, %
Inoculum	4.1×10^6		4.3×10^6		1.8×10^6		1.8×10^6	
COG	8.0×10^5		3.0×10^5		2.7×10^4		2.3×10^4	
COG-PE	7.7×10^5	3.75	2.8×10^5		3.2×10^4		1.0×10^4	
COG-AA	6.9×10^5	13.8	3.5×10^5		2.9×10^4		3.0×10^4	
COG-Ag-PE	6.4×10^5	20.0	400	99.9	0	100	0	100
COG-Ag-AA	1.6×10^5	80.5	500	99.9	2.9×10^2	98.9	0	100

Cotton gauze containing Ag NPs as a potential medical textile should be in direct contact with human skin and bodily fluids (blood or lymph). Therefore, understanding the properties of the NPs and their effects on the body and bodily fluids is crucial. To simulate body fluid, a physiological saline solution was selected as a release medium, as its salinity is close to that of blood or lymph. Fig.

7 illustrates the amounts of Ag^+ ions released from samples in the physiological saline solution within 24 hours. A larger amount of Ag^+ ions was released from the COG-Ag-AA sample compared to the COG-Ag-PE sample. This supports the assumption that some amount of Ag^+ ions is loosely bound to the cotton fibers in the COG-Ag-AA sample. The maximum amount of Ag^+ ions released from the COG-Ag-PE and COG-Ag-AA samples in the physiological solution was 0.714±0.003 and 1.025±0.020 μmol/g, respectively. An analysis of the total amount of silver in the COG-Ag-PE and COG-Ag-AA samples, in conjunction with the maximum release of Ag^+ ions after 24 hours, revealed that approximately 95% and 92% of the silver was retained in the samples, respectively. These findings are comparable to cotton samples with Ag-based NPs synthesized in the presence of *Juglans regia* and *Humulus lupulus* extracts.[26]

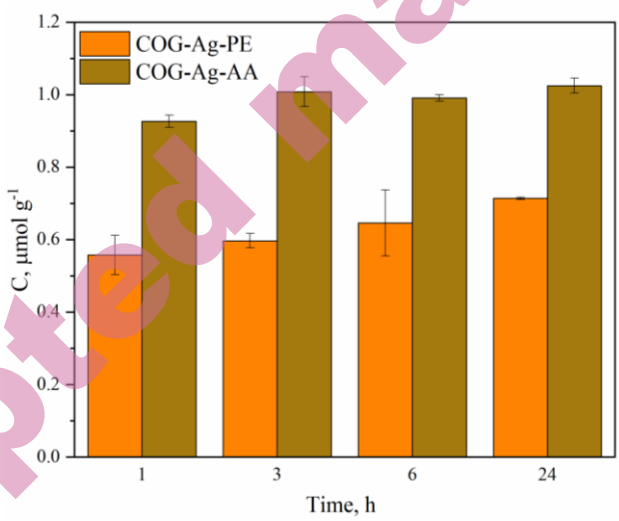

Fig. 7. Release of Ag^+- ions from the samples into physiological saline solution

CONCLUSION

This study revealed that extracts from *P. euramericana* and *A. altissima* leaves could be utilized for the synthesis of Ag-based NPs on cotton gauze. FESEM analysis and EDS mapping showed that spherical, mostly single Ag-based NPs were evenly distributed across the surface of the cotton fibers. The total amount of silver in the samples, the size and shape of the NPs, negligibly depend on the applied plant extracts. Even though the total silver content is similar, a higher number of nanoparticles with larger sizes was detected in the sample derived from *P. euramericana* extract, suggesting that a certain amount of silver ions was only adsorbed onto the samples synthesized using *A. altissima* (Mill.) Swingle leaves extract. Antibacterial tests revealed time-dependent antibacterial activity.

However, the concentration of silver in all samples was sufficient to provide excellent antibacterial activity against *E. coli* and *S. aureus* after 24 hours. Release studies demonstrated that 92-95% of silver was retained in the samples after a 24-hour exposure to a physiological saline solution, suggesting a high level of stability in the samples.

Acknowledgements: This work was financially supported by the Ministry of Science, Technological Development, and Innovation of the Republic of Serbia (Contract No. 451-03-136/2025-03/200017, 451-03-136/2025-03/200135 and 451-03-136/2025-03/200003). The authors appreciate Prof. dr. Slobodan D. Milanović from the Faculty of Forestry, University of Belgrade, for collecting *A. altissima* leaves.

И З В О Д

ОДРЖИВА СИНТЕЗА НАНОЧЕСТИЦА СРЕБРА НА ПАМУЧНОЈ ГАЗИ ЗА ПОБОЉШАНА АНТИБАКТЕРИЈСКА СВОЈСТВА

ДАРКА Д. МАРКОВИЋ[1*], ВАЊА Б. ТАДИЋ[2], АНА Р. ЖУГИЋ[2], МАЈА М. РАДЕТИЋ[3]

[1]Универзитет у Београду, Институт за нуклеарне науке „Винча“- Институт од националног значаја, Михајла Петровића Аласа 12-14, Београд, Србија, [2]Универзитет у Београду, Институт за проучавање лековитог биља „Јосиф Панчић“, Тадеуша Кошћушка 1, 11000 Београд, Србија, и [3]Универзитет у Београду, Технолошко-металуршки факултет, Карнегијева 4, 11000 Београд, Србија.

Заштита рана је кључни корак у превенцији или смањењу инфекција, као и преношења инфекција између пацијената. Завоји за ране су неопходни медицински производи који покривају ране и олакшавају зарастање. У овом раду се испитује могућност коришћења наночестица сребра за обезбеђивање антибактеријске активности памучној гази, често коришћеном материјалу за једнократну употребу за завоје за ране. *In situ* синтеза наночестица на бази сребра на памучној гази постигнута је коришћењем екстраката из листова *Populus x euramericana* (PE) и *Ailanthus altissima (Mill.) Swingle* (AA). Главна фитохемијска једињења у екстрактима су квантификована помоћу HPLC-a. FESEM и EDS анализа мапирања површине потврдиле су присуство наночестица на бази сребра на површини влакана оба узорка. Просечна величина наночестица синтетизованих у присуству екстраката PE и AA износила је 88±26 nm односно 82±23 nm. Сличан садржај сребра пронађен је у узорку добијеном са екстрактом PE (14,22±0,23 μmol/g) у поређењу са узорком синтетисаним коришћењем екстракта AA (13,63±1,40 μmol/g). Синтетизовани узорци остварују максималну редукцију Грам-негативних бактерија *Escherichia coli* и Грам-позитивних бактерија *Staphylococcus aureus*.

(Примљено 3. јуна; ревидирано 15. јула; прихваћено 23. септембра 2025.)

REFERENCES

1. F. Feng, Z. Zhao, J. Li, Y. Huang, W. Chen, *Prog. Mat. Sci*. **146** (2024) 101328 (https://doi.org/10.1016/j.pmatsci.2024.101328)
2. S. Lv, Y. Liu, C. Liu, J. Yin, D. An, S. Deng, G. Liu, *Ind. Crop. Prod*. **224** (2025) 120384 (https://doi.org/10.1016/j.indcrop.2024.120384)
3. U. L. Bristi, A. Rahman, S. B. Malitha, O. Rahman, S. Shoukat, *Sci. Rep*. **14** (2024) 31650 (https://doi.org/10.1038/s41598-024-80318-0)

4. O. S Boateng, K. H. Matthews, H. N. E. Stevens, G. M. Eccleston, *J. Pharm. Sci.* **97** (2008) 2892 (https://doi.org/10.1002/jps.21210)
5. K. Rahim, S. Saleha, X. Zhu, L. Huo, A. Basit, O. L. Franco, *Microb. Ecol.* **73** (2017) 710 (https://doi.org/10.1007/s00248-016-0867-9)
6. M. M. Mihai, M. Preda, I. Lungu, C. M.Gestakl, M. I. Popa, A. Holban, *Int. J. Mol. Sci.* **19** (2018) 1179 (https://doi.org/10.3390/ijms19041179)
7. A. Hanczvikkel, A. Víg, A. Tóth, *J. Ind. Text.* **48** (2019) 1113 (https://doi.org/10.1177/1528083718754901)
8. C. Z. Bueno, A. M. Moraes, *Mat. Sci. Eng. C* **93** (2018) 671 (https://doi.org/10.1016/j.msec.2018.07.076)
9. A. Basu, K. Heitz, M. Strømme, K. Welch, N. Ferraz, *Carbohydr. Polym.* **181** (2018) 345 (https://doi.org/10.1016/j.carbpol.2017.10.085)
10. G. Liu, J. Xiang, Q. Xia, K. Li, T. Lan, L. Yu, *Cellulose* **26** (2019) 1383 (https://link.springer.com/article/10.1007/s10570-018-2110-y)
11. Y. Dai, H. Li, J. Wan, L. Liang, J. Yan, *Ind. Crop. Prod.* **208** (2024) 117871 (https://doi.org/10.1016/j.indcrop.2023.117871)
12. B. Simončič, B. Tomšič, *Text. Res. J.* **80** (2010) 1721 (https://doi.org/10.1177/0040517510363193)
13. M. Radetić, *J. Mater. Sci.* **48** (2013) 95 (https://doi.org/10.1007/s10853-012-6677-7)
14. V. Bhandari, S. Jose, P. Badanayak, A. Sankaran, V. Anandan, *Ind. Eng. Chem. Res* **61** (2022) 86 (http://dx.doi.org/10.1021/acs.iecr.1c04203)
15. S. Milovanovic, M. Stamenic, D. Markovic, M. Radetic, I. Zizovic, *J. Supercritical Fluids* **84** (2013) 173 (http://dx.doi.org/10.1016/j.supflu.2013.10.003)
16. R. Nawaz, S. T. R. Naqvi, B. Fatima, N. Zulfiqar, M. U. Farooq, M. N. ul Haq, D. Hussain, A. Javeed, A. Rasul, L. Jafri, S.t Majeed, W. Q. Khan, *Sci. Rep*. **12** (2022) 2493 (https://doi.org/10.1038/s41598-022-06391-5)
17. S. Srisod, K. Motina, T. Inprasit, P. Pisitsak, *Prog. Org. Coat*. **120** (2018) 123 (https://doi.org/10.1016/j.porgcoat.2018.03.007)
18. A. M. Abdelgawad, E. Shaban, D. A. Elsherbiny, R. A. El-Sherbiny, H. Farouk, I. El-Tantawy El-Sayed, *Fib. Polym.* **26** (2025) 1223 (https://doi.org/10.1007/s12221-025-00880-w)
19. M. Khan, M. R. Shaik, S. F. Adil, S. T. Khan, A. Al-Warthan, M. H. Siddiqui, M. N. Tahir, W. Tremel, *Dalton Trans*. **47** (2018) 11988–12010 (https://doi.org/10.1039/c8dt01152d)
20. M.A. Kakakhel, W. Sajjad, F. Wu, N. Bibi, K. Shah, Z. Yali, W. Wang, *J. Hazard. Mater. Adv.* **1** (2021) 100005 (https://doi.org/10.1016/j.hazadv.2021.100005)
21. A. Soleimani-Gorgani, O. Avinc, R. Alborz, *J. Clean. Prod.* **386** (2023) 135796 (https://doi.org/10.1016/j.jclepro.2022.135796)
22. M. Maghimaa, S. A. Alharbi, *J. Photoch. Photobio. B* **204** (2020) 111806 (https://doi.org/10.1016/j.jphotobiol.2020.111806)
23. Z. Yu, J. Liu, H. He, Y.Wang, Y. Zhao, Q. Lu, Y. Qin, Y. Ke, Y. Peng, *Cellulose* **28** (2021) 1827 (https://doi.org/10.1007/s10570-020-03639-z)
24. N. Čuk, M. Šala, M. Gorjanc, *Cellulose* **28** (2021) 3215 (https://doi.org/10.1007/s10570-021-03715-y)
25. D. Štular, E. Savio, B. Simončič, M. Šobak, I. Jerman, I. Poljanšek, A. Ferri, B. Tomšič, *Appl. Surf. Sci.* **563** (2021) 150361 (https://doi.org/10.1016/j.apsusc.2021.150361)

26. A. Krkobabić, M. Radetić, A. Zille, A. I. Ribeiro , V. Tadić , T. Ilic-Tomic, D. Marković, *Molecules* **29** (2024) 1447 (https://doi.org/10.3390/molecules29071447)
27. A. Krkobabić, M. Radetić, H.H. Tseng, T.S. Nunney, V. Tadić, T. Ilic-Tomic, D. Marković, *Appl. Surf. Sci*. **611** (2023) 155612 (https://doi.org/10.1016/j.apsusc.2022.155612)
28. W. Ding, H. Li, J. Wen, *Ecol. Ind.* **143** (2022) 109408 (https://doi.org/10.1016/j.ecolind.2022.109408)
29. M. Arshad, A. Khan, Z. H. Farooqi, M. U. M. A. Waseem, S. A. Shah, M. Khan, *Mat. Sci.-Pol.* **36** (2018) 21 (https://dx.doi.org/10.1515/msp-2017-0100)
30. Y.S. Velioglu, G. Mazza, L. Gao, B.D. Oomah, *J. Agricul. Food Chem.* **46** (1998) 4113 (https://doi.org/10.1021/jf9801973)
31. European Pharmacopeia, 11th ed.; Council of Europe: Strasbourg, France, 2023
32. S. S. R. Albeladi, M. A. Malik, S. A. Al-thabaiti, *J. Mat. Res. Tech*. **9** (2020) 10031 (https://doi.org/10.1016/j.jmrt.2020.06.074)
33. C. Tamuly, M. Hazarika, S. Ch. Borah, M. R. Das, M. P. Boruah, *Colloids Surf. B Biointerfaces* **102** (2013) 627 (https://doi.org/10.1016/j.colsurfb.2012.09.007)
34. N. Ahmad, S. Bhatnagar, S. S. Ali, R. Dutta, *Int. J. Nanomed.* **10** (2015) 7019 (https://doi.org/10.2147/ijn.s94479)
35. V. Ilić, Z. Šaponjić, V. Vodnik, B. Potkonjak, P. Jovančić, J. Nedeljković, M. Radetić, *Carbohydr. Polym.* **78** (2009) 564 (https://dx.doi.org/10.1016/j.carbpol.2009.05.015)
36. A. Krkobabić, D. Marković, A. Kovačević, V. Tadić, M. Radoičić, T. Barudžija, T. Ilic-Tomic, M. Radetić, *Fib. Polym.* **23** (2022) 954-966 (https://doi.org/10.1007/s12221-022-4639-5)
37. C. Chung, M. Lee, E. Choe, *Carbohyd. Polym*. **58 (**2004) 417 (https://doi.org/10.1016/j.carbpol.2004.08.005)
38. N. Durán, M. Durán, M. B. de Jesus, A. B. Seabra, W. J. Fávaro, G. Nakazato, *Nanomed. Nanotechnol. Biol. Med.* **12** (2016) 789 (http://dx.doi.org/10.1016/j.nano.2015.11.016).
39. C. M.Crisan, T. Mocan, M. Manolea, L. I. Lasca, F. A. Tbăran, L. Mocan, *Appl. Sci.* **11** (2021) 1120 (https://doi.org/10.3390/app11031120).
40. I. S. Sandí, S. C. Fuentes, R. P. Reyes, J. R. V. Baudrit, D. B. Menezes, G. M. O. Vásquez, *Biotechnol. Rep.* **40** (2023) e00816 (https://doi.org/10.1016/j.btre.2023.e00816).
41. L. Hochvaldová, D. Panáček, L. Válková, R. Večeřová, M. Kolář, R. Prucek, L. Kvítek, A. Panáček, *Commun. Biol.* **7** (2024) 1552 (https://doi.org/10.1038/s42003-024-07266-3).